



# Electrospun protein fibers as matrices for tissue engineering

Mengyan Li<sup>a</sup>, Mark J. Mondrinos<sup>a</sup>, Milind R. Gandhi<sup>a</sup>, Frank K. Ko<sup>b</sup>,  
Anthony S. Weiss<sup>c</sup>, Peter I. Lelkes<sup>a,\*</sup>

<sup>a</sup>*School of Biomedical Engineering, Science and Health Systems, Drexel University, USA*

<sup>b</sup>*Department of Materials Science and Engineering, College of Engineering, Drexel University, USA*

<sup>c</sup>*School of Molecular and Microbial Biosciences, University of Sydney, Australia*

Received 6 November 2004; accepted 23 March 2005

## Abstract

Electrospinning has recently emerged as a leading technique for generating biomimetic scaffolds made of synthetic and natural polymers for tissue engineering applications. In this study, we compared collagen, gelatin (denatured collagen), solubilized alpha-elastin, and, as a first, recombinant human tropoelastin as biopolymeric materials for fabricating tissue engineered scaffolds by electrospinning. In extending previous studies, we optimized the shape and size (diameter or width)<sup>1</sup> of the ensuing electrospun fibers by varying important parameters of the electrospinning process, such as solute concentration and delivery rate of the polymers. Our results indicate that the average diameter of gelatin and collagen fibers could be scaled down to 200–500 nm without any beads, while the alpha-elastin and tropoelastin fibers were several microns in width. Importantly, and contrary to any hitherto reported structures of electrospun polymers, fibers composed of alpha-elastin, especially tropoelastin, exhibited “quasi-elastic” wave-like patterns at increased solution delivery rates. The periodicity of these wave-like tropoelastin fibers was partly affected by the delivery rate. Atomic force microscopy was utilized to profile the topography of individual electrospun fibers and microtensile testing was performed to measure their mechanical properties. Cell culture studies confirmed that the electrospun engineered protein scaffolds support attachment and growth of human embryonic palatal mesenchymal (HEPM) cells.

© 2005 Elsevier Ltd. All rights reserved.

**Keywords:** Electrospinning; Nanofibers; Gelatin; Collagen; Elastin; Tropoelastin

## 1. Introduction

The ability of cells to build tissues and maintain tissue-specific functions critically depends on epigenetic factors, such as the unique cell/tissue-specific microenvironment. Some of the major factors contributing to this unique microenvironment are cell–cell interactions and the organotypic extracellular matrix (ECM). Interactions between cells and ECM are crucial to cellular differentiation and in modulating or redirecting cell function [1–6]. However, as the cells are removed from their microenvironment and cultured in an in vitro environment, they typically dedifferentiate, thereby losing some of their normal in vivo behavior. A principal objective of tissue engineering, therefore, is to recreate in an in vitro culture system some of the

**Abbreviations:** AFM, atomic force microscope; DMEM, Dulbecco's Modified Eagle's Medium; ECM, extracellular matrix; HEPM, human embryonic palatal mesenchymal; HFP, 1, 1, 1, 3, 3, 3 Hexafluoro-2-Propanol; HMDI, 1, 6-diisocyanatohexane; P(LLA-CL), poly(L-lactide-co-ε-caprolactone); PCL, poly(ε-caprolactone); PGA, poly(glycolic acid); PLA, poly(lactic acid); PLGA, poly(lactide-co-glycolide); SEM, scanning electron microscope; TCPS, tissue-culture treated polystyrene.

\*Corresponding author. Calhoun Chair Professor of Cellular Tissue Engineering, School of Biomedical Engineering, Science and Health Systems, Drexel University, New College Building, 245 N. 15th Street, Philadelphia, PA 19102, USA. Tel.: +1 215 762 2071; fax: +1 215 895 4983.

E-mail address: [pillelkes@drexel.edu](mailto:pillelkes@drexel.edu) (P.I. Lelkes).

<sup>1</sup>Diameter is used to describe the rounded gelatin and collagen fibers and width is used to describe the ribbon-like elastin and tropoelastin fibers.

essential factors in the cellular microenvironment which control and regulate cell function *in vivo*.

The process of electrospinning, well known for many years in the textile industry and in organic polymer science [7–10], has recently re-emerged as a novel tool for generating biopolymer scaffolding for tissue engineering [11]. Specifically, electrospinning provides a mechanism to produce nanofibrous scaffolds from a variety of polymer materials, including synthetic polymers and natural proteins. The topology of these electrospun scaffolds closely mimics that of native ECM. Fibers with diameters in the range from several micrometers down to less than 100 nm have a very high surface area to mass ratio, and can be electrospun into 3-D scaffolds with very high porosity. In this way, biomimetic matrices can be fabricated by electrospinning which facilitate cell attachment, support cell growth, and regulate cell differentiation [12].

To date, electrospinning has been applied for the fabrication of nanofibrous scaffolds from numerous biodegradable polymers, such as poly( $\epsilon$ -caprolactone) (PCL), poly(lactic acid) (PLA), poly(glycolic acid) (PGA), and the copolymer poly(lactide-*co*-glycolide) (PLGA) [13–16]. These biodegradable polymers have been used to electrospin engineered scaffolds for bone tissue [17–19] and cardiac grafts [20]. Similarly, poly(L-lactide-*co*- $\epsilon$ -caprolactone) [P(LLA-CL)] has been electrospun into nanofibrous scaffolds for engineering blood vessel substitutes [21,22]. Polyurethane (PU) nanofibrous membranes have been used as wound dressings [23].

Collagen and elastin are two of the key structural proteins found in the extracellular matrices of many tissues [24,25]. These proteins are important modulators for the physical properties of any engineered scaffold, affecting cellular attachment, growth and responses to mechanical stimuli [26–28]. Huang and coworkers were the first to electrospin collagen scaffolds for wound dressing [29,30]. Shortly thereafter, Matthews et al. [31] and Boland et al. [32] described electrospinning of collagen and elastin fibers for preliminary vascular tissue engineering. However, the detailed mechanical properties of electrospun collagen and elastin fibers have not yet been described.

Tropoelastin is secreted from elastogenic cells as a 60 kDa monomer that is subjected to oxidation by lysyl oxidase. Subsequent protein–protein associations give rise to massive macroarrays of elastin. As a consequence, elastin is a substantially insoluble protein network that displays elasticity, resilience and biological persistence. Soluble material is typically derived either as fragmented elastin in the form of alpha- and kappa-elastin [33] or preferably through expression of the natural monomer tropoelastin [34] that as of yet have not been electrospun.

In this study, we compared the properties of electrospun fibers made of gelatin (denatured collagen), collagen,

solubilized alpha-elastin, and, as a first, recombinant human tropoelastin. The electrospinning parameters were optimized to achieve smooth, uniform fibers free of beads. In contrast to collagen and gelatin, which could be spun into fibers in the nanometer scale, the diameter of alpha-elastin and tropoelastin fibers was always in the range of microns. These latter fibers appeared flattened and exhibited “quasi-elastic” wave-like patterns at increased delivery rates of polymer solutions. We also report the characterization of the mechanical tensile moduli of electrospun gelatin, collagen, alpha-elastin, and tropoelastin fibers. Finally, the usefulness of these fibrous matrices as scaffolds for tissue engineering purposes was ascertained by assessing the attachment and proliferation of human embryonic palatal mesenchymal (HEPM) cells.

## 2. Material and methods

### 2.1. Materials

Gelatin (bovine skin, type B powder), collagen (calf skin, type I powder), alpha-elastin (soluble bovine, lyophilized powder) were purchased from Sigma (St. Louis, MO). The synthesis and characterization of recombinant human tropoelastin has previously been reported [33,35]. For electrospinning, all proteins were dissolved in 1,1,1,3,3,3 Hexafluoro-2-Propanol (HFP). Unless noted otherwise, all chemicals and reagents were purchased from Sigma-Aldrich.

### 2.2. Electrospinning

Electrospinning was carried out according to the procedure essentially as detailed by Li et al. [13]. Briefly, protein solutions were loaded into 5 ml plastic syringes (BD Biosciences) equipped with blunt 18 gauge needles. The syringes were then placed in a syringe pump (14-831-1, KD Scientific Single-Syringe Infusion Pump, Fisher Scientifics) and the needles connected to the positive output of a high voltage power supply (ES30-0.1P, Gamma High Voltage Research Inc.). Fibers were electrospun onto circular cover glasses (18 mm  $\varnothing$ , Fisher Scientifics) which were attached to a brass grounded target (25 mm  $\times$  75 mm). The delivery rates were tested at a range of 1–10 ml/h. Electrospinning was carried out with the high voltage power supply set at 10 kV with an air gap distance of 15 cm. The concentrations of gelatin/collagen and elastin/tropoelastin were 8.3% and 20% (w/v), respectively, except as otherwise specified.

### 2.3. Crosslinking

For cell culture, electrospun protein fibers were crosslinked with 10% (by volume) HMDI (1,6-diisocyanatohexane) in isopropanol for 1 h at room

temperature (Weiss, A.S., unpublished). The scaffolds were then rinsed in isopropanol for 2 min to remove the residual of crosslinker. Finally, the fibers were soaked in distilled water for 1 h and dried overnight in an oven at 50 °C.

#### 2.4. Cell culture

HEPM cells (American Type Culture Collection, ATCC, CRL-1486, [36]) were used for the initial assessment of attachment and migration on electrospun protein fibers. These cells were routinely maintained in Eagle's MEM with Earle's salts supplemented with 10% fetal bovine serum (Hyclone), 2.0 mM L-glutamine, 1.0 mM sodium pyruvate, 0.1 mM non-essential amino acids, and 1.5 g/L sodium bicarbonate at 37 °C in a 5% CO<sub>2</sub> incubator.

Upon crosslinking, the scaffolds were sterilized in 70% ethanol for 1 h followed by three rinses with 1 × phosphate buffered saline (PBS). HEPM cells were seeded onto the various fibrous scaffolds at a density of 20,000 cells/sample. Following 2 h for attachment in Dulbecco's Modified Eagle's Medium (DMEM), the initial seeding efficiency was assessed using the Alamar telue (AB) (Biosource) assay [37,38]. For continual assessment of cell proliferation, the AB assay was performed for up to 6 days. After termination of each experiment, the samples were fixed with 10% buffered formalin for 1 h at room temperature and then left overnight in PBS at 4 °C. The samples were washed once, and the cells permeabilized for 15 min in PBS containing 25 µg/ml digitonin (Sigma) [39]. Following a gentle wash in PBS, the samples were incubated for 15 min in PBS containing 2 µg/ml Hoechst 33258 (Bis-benzimide), a nuclear stain, and 1 µg/ml rhodamine-phalloidin (Phalloidin Tritc-labeled), a specific stain for microfilaments.

#### 2.5. Microscopic analysis

For analysis of the morphology of the electrospun fibers, the samples were sputter-coated with Au/Pd and examined with a scanning electron microscope (SEM, XL-30 Environmental SEM-FEG). Each micrograph from an SEM scan was digitized. The average fiber diameter and the periodicity of elastin/tropoelastin fibers were calculated using UTHSCSA ImageTool 3.0 imaging software. Fiber surface topographies were inspected with an atomic force microscope (AFM, Multimode SPM, Veeco).

#### 2.6. Microtensile test

The tensile properties of electrospun 3-D fibrous protein scaffolds, approximately 0.2–0.5 mm × 5 mm × 25/50 mm ( $H \times W \times L$ ), were characterized using a

Kawabata Evaluation System (KES-G1, Kato Tech Co., Japan) according to routine mechanical testing methods for fabric materials [13]. The ends of the rectangular specimens were mounted vertically on two 1 cm × 1 cm mechanical gripping units of the tensile tester, leaving a 15/40 mm gauge length for mechanical loading. An extension rate of 0.2 mm/s, sensitivity of 5 × 10<sup>10</sup> V = 1000 g, and frequency of 50 Hz were used in the tensile tests. Load-deformation data were recorded and the stress–strain curve of the fibrous structure was constructed from the load-deformation curve. The specific stress in gm/tex was calculated using the following equation:

$$\text{Stress (gm/tex)} = \frac{\text{Force (gm)}}{\text{Areal density (gm/m}^2\text{)} \times \text{width (mm)}} \quad (1)$$

The areal density is the weight (gm) of the tested strip of the specimen divided by the length (m) and width (m) of the test specimen. The specific stress in gm/tex, where tex = Kg/1000 m, can be converted to SI unit MPa by taking the density of the specimen into consideration and the strain was calculated by dividing the displacement by the gauge length in mm.

#### 2.7. Statistical analyses

The number of independent replication is listed individually for each experiment. Where applicable, all data are expressed as mean ± standard deviation. Linear regression analysis, Student's *t*-test, and single factor ANOVA were used for parameter estimation and hypothesis testing, with  $p < 0.05$  considered as being statistically significant.

### 3. Results and discussion

#### 3.1. Characterization of electrospinning processing parameters

As previously reported, the concentration of the polymer solution, applied voltage, air gap distance, and delivery rate are critical experimental processing variables which determine the shape and size of electrospun fibers [11,16,31]. In this study, the effects of the processing parameters were investigated to produce the desirable electrospun protein fibers. For economic reasons, most of the preliminary studies optimizing the electrospinning parameters of biological ECM-derived molecules were carried out with gelatin rather than with collagen, alpha-elastin, and tropoelastin. However, all critical parameters used also validated with these other proteins.

To investigate the concentration effect, the solution delivery rate was kept constant at 5 ml/h. The applied

voltage and air gap distance were varied in the range of 10–15 kV and 10–20 cm, respectively. As shown in Fig. 1, by decreasing the concentration of gelatin in the solvent HFP from 8.3% to 2%, the average size of gelatin fibers was reduced from  $485 \pm 187$  nm to  $77 \pm 41$  nm ( $p < 0.01$ ). The most drastic decrease in fiber diameter, i.e., from  $\sim 500$  to  $\sim 200$  nm, occurred when the initial gelatin concentration was reduced to 5%. Further reduction in gelatin concentration reduced the fiber size to below 100 nm. However, this reduction of fiber size was accompanied by a significant formation of beads. There were very few beads in the 5% gelatin fibers; gelatin fibers electrospun at the concentration of 8.3% were entirely devoid of beads. Similar results were obtained for electrospun collagen fibers. These results are comparable to the results reported by Boland et al. [32] for electrospun type I collagen fibers with average fiber diameters ranging from  $\sim 100$  nm to  $4.6 \mu\text{m}$  depending on the concentration. In line with previous reports on other polymeric materials [40], we conclude that electrospinning of collagenous proteins at concentrations above 5% will yield smooth and uniform fibers of several hundred nanometers in diameters. By contrast, electrospinning at lower concentrations will result in small fibers, but with beads.

The width of electrospun alpha-elastin fibers also depended on the concentration of the solution, the dose response curve, however, was significantly right-shifted. As seen in the SEM micrographs in Fig. 2(a), electrospinning of alpha-elastin at 10% (w/v), the lowest concentration tested, yielded large beads and fragmented fibers. At 15%, there were no more beads, but the fibers were still fragmented. When raising the alpha-elastin concentration to 20%, the electrospun fibers were continuous and more uniform as shown in Fig. 2(b).

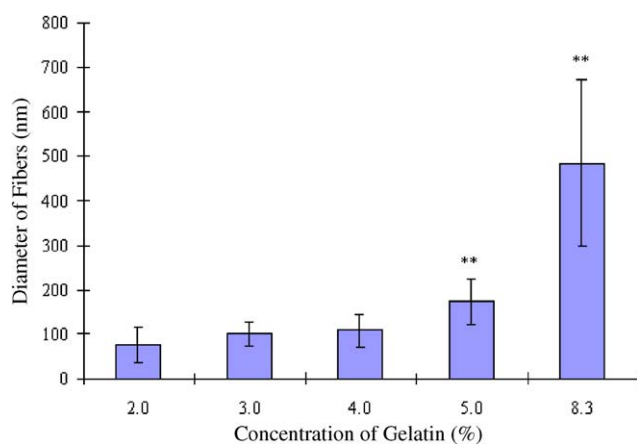


Fig. 1. Sizes of electrospun gelatin fibers at different concentrations (electrospun fibers were examined by SEM, the fiber size evaluated by ImageTool3. Data are expressed as means  $\pm$  SD,  $n = 20$ – $30$ , \*\*  $p < 0.01$ , values are significantly different from the previous group compared).

Significantly, alpha-elastin fibers electrospun at 20% concentration were evidently wider than those at 10% and 15%. These results agree with the previous investigations reported by Buchko et al. [11] for silk-like polymers with fibronectin functionality. Generally, alpha-elastin and tropoelastin fibers had larger sizes than gelatin and collagen fibers.

In the next set of experiments, we investigated the effects of the delivery rate on the size and, specifically for elastin, the periodicity of biopolymeric protein fibers. Based on our preliminary results, three of the electrospinning parameters were kept constant: concentration (8.3% for gelatin and collagen, 20% for alpha-elastin and tropoelastin), applied voltage (10 kV) and air gap distance (15 cm). We then systematically varied the delivery rates of the protein solutions between 1 and 8 ml/h in order to optimize the conditions that yield bead-free and uniform fibers.

Increasing the delivery rate from 1 to 3 ml/h yielded a significant ( $p < 0.01$ ) change in fiber diameter from  $431 \pm 105$  nm to  $533 \pm 119$  nm, from  $349 \pm 97$  nm to  $460 \pm 148$  nm for collagen and gelatin, respectively. A further increase in the rate of delivery from 3 to 8 ml/h did not significantly change the mean size (diameter) of collagen (from  $533 \pm 119$  nm to  $577 \pm 146$  nm) and gelatin (from  $460 \pm 148$  nm to  $517 \pm 241$  nm) fibers ( $p > 0.05$ ). Statistical analysis of the dose dependence revealed a better fit for logarithmic regression ( $R^2 = 0.87$  and  $0.97$ , respectively) (Fig. 3a) than for linear regression ( $R^2 = 0.79$  and  $0.82$ , respectively). By contrast, for alpha-elastin and even more for tropoelastin, which intrinsically yielded wider fibers than collagen or gelatin, the widths of the ensuing fibers were strongly affected by the delivery rate. Increasing the delivery rate from 1 to 8 ml/h, the mean width of the fibers increased approximately seven-fold, from  $0.6 \pm 0.1 \mu\text{m}$  to  $3.6 \pm 0.7 \mu\text{m}$  (alpha-elastin), and from  $1.4 \pm 0.3 \mu\text{m}$  to  $7.4 \pm 2.3 \mu\text{m}$  (tropoelastin), respectively ( $p < 0.01$ ). The linear regression indicated significance for the dose-dependence of alpha-elastin and tropoelastin on the delivery rates in Fig. 3b ( $R^2 = 0.987$  and  $0.998$ , respectively). Our data for the width of electrospun elastin fibers are comparable to the size of electrospun bovine neck ligament elastin fibers of  $1.1 \pm 0.7 \mu\text{m}$  reported by Boland et al. [32]. The thickness of ribbon-like tropoelastin fibers was approximately 500–700 nm for a 7.5- $\mu\text{m}$ -wide fiber (Fig. 3c and d). As most of the ribbon-like fibers were not standing vertically on the substrate, the exact measurement of the width of elastin fibers was not always possible; thus we can only provide an approximate range of dimensions rather than listing means and standard deviations for their thickness. Interestingly, electrospun tropoelastin fibers are always 2–3 times wider than fibers spun under identical conditions from alpha-elastin. As a caveat, we noticed that by increasing the delivery rate

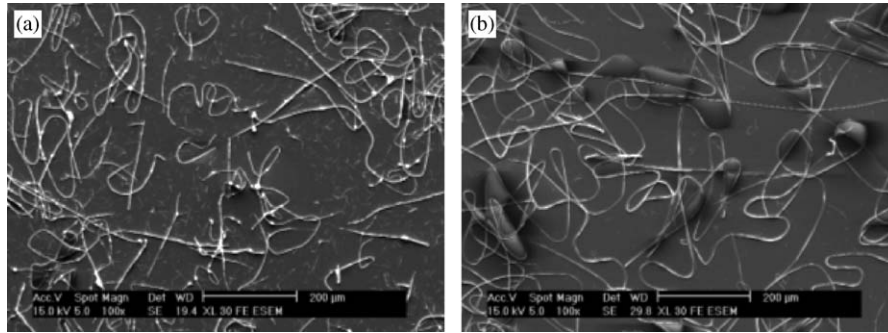


Fig. 2. SEM micrographs of electrospun elastin fibers at different concentrations. (a) 10%; (b) 20%. Original magnifications are  $100\times$ . Figure shows the electrospun elastin fibers were more uniform when increasing concentration from 10% to 20%.

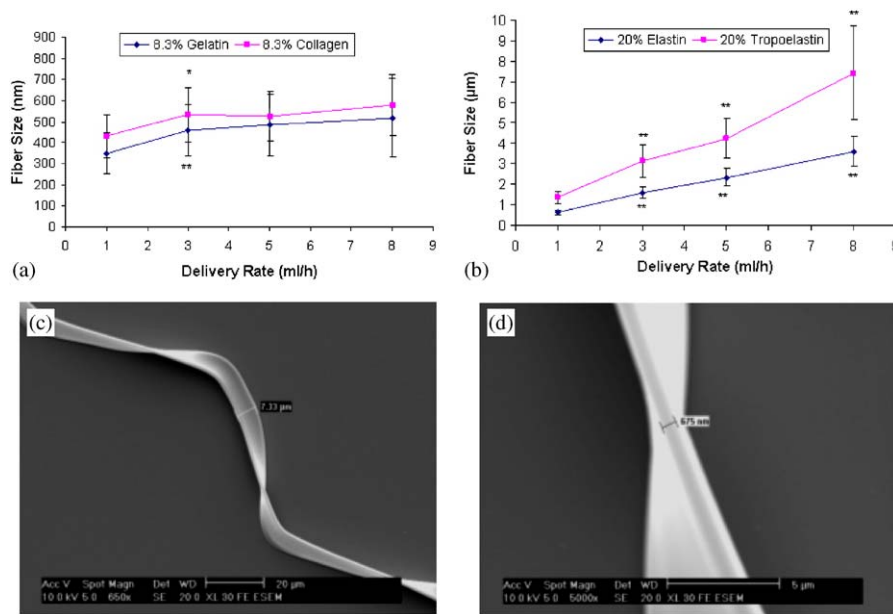


Fig. 3. Comparison of electrospun gelatin/collagen and elastin/tropoelastin fibers. (a) Sizes of electrospun gelatin and collagen fibers at different delivery rates. (b) Sizes of electrospun elastin and tropoelastin fibers at different delivery rates. (c) and (d) SEM micrographs of 20% tropoelastin fibers electrospun at 5 ml/h, showing the width and thickness of ribbon-like tropoelastin fibers, original magnifications are  $650\times$  and  $5000\times$ , respectively. (Data are expressed as means  $\pm$  SD,  $n = 20-30$ , \*  $p < 0.05$ ; \*\*  $p < 0.01$ , values are significantly different from the previous group compared).

above a certain threshold, 3 ml/h, the production of beads for collagen and gelatin also increased, while alpha-elastin and tropoelastin fibers became “wet” and flattened at delivery rates above 5 ml/h. Therefore, uniform fibers could only be achieved by tightly controlling the solution delivery rate in a material-specific range.

In addition to intrinsic differences in fiber sizes, close examination of the scanning electron micrographs also indicated significant differences in the topology of the fibers spun from collagenous proteins and from elastin/tropoelastin. As seen in the SEM and AFM micrographs in Fig. 4, both gelatin and collagen fibers appear uniformly round when formed at 1 ml/h. By contrast, under the same experimental conditions, alpha-elastin as

well as tropoelastin fibers appear wider and flatter, shaped like ribbons, with their size resembling that of naturally occurring elastin fibers [41]. Analysis by AFM indicates that the elastin/tropoelastin ribbons exhibit a symmetric increase in their thickness at the edges (Fig. 4d). With increasing delivery rates, alpha-elastin and tropoelastin fibers became much wider (more than  $10\ \mu\text{m}$  in width, Fig. 4e); a similar phenomenon was also seen for collagen and elastin fibers at the higher delivery rates (figure not shown). The ribbon shape of electrospun elastin and tropoelastin is independent of the delivery rate and appears to be innate, as it is also observed in situ native blood vessels [42,43]. By contrast, the formation of ribbon-shaped collagen and gelatin fibers at high solute concentrations and delivery rates

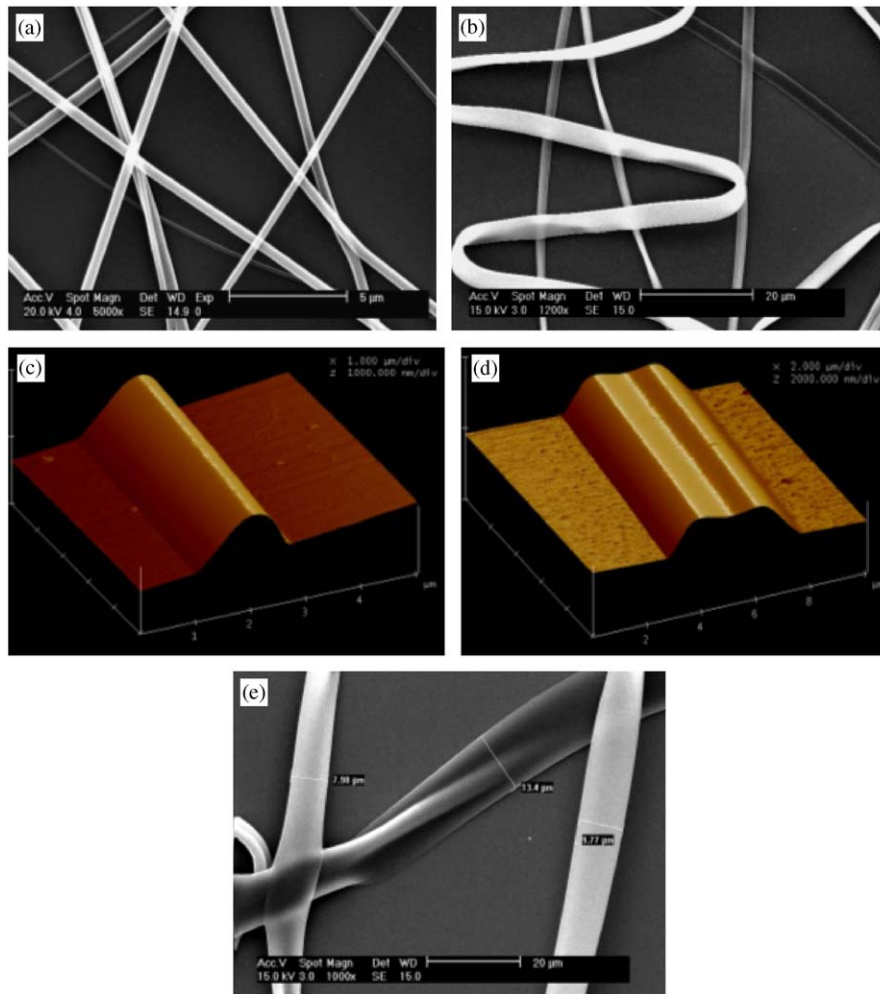


Fig. 4. Comparison of electrospun collagen and tropoelastin fibers by SEM and AFM micrographs. (a) SEM micrograph of collagen fibers, magnification is  $5000\times$ . (b) SEM micrograph of tropoelastin fibers, magnification is  $1200\times$ . (c) AFM image of collagen fiber, showing the round shape of the fiber. (d) AFM image of tropoelastin, showing the ribbon shape of the fiber. (e) SEM micrograph of tropoelastin fibers, magnification is  $1000\times$ , showing the wider fibers at higher delivery rate.

may be due to slow solidification and/or solvent evaporation after landing on the target. It remains to be tested whether differences in the shapes of these protein fibers will influence cell growth on scaffolds engineered from these diverse materials.

In situ, elastin has a wave-like periodic appearance in the larger elastic arteries [43,44]. Interestingly, the innate elastic properties of alpha-elastin and tropoelastin are retained upon electrospinning (see Figs. 2 and 4): at a delivery rate of 1.5 ml/h, fibers made of alpha-elastin and tropoelastin were significantly different from gelatin and collagen fibers, in that alpha-elastin and tropoelastin fibers attained an elastic, wavy pattern, while collagen and gelatin fibers were mostly straight. These differences in fiber topology were clearly visible when observing fibrous mats made of electrospun collagen and elastin fibers and using their autofluorescence (Fig. 5).

Close inspection of SEM micrographs of wavy tropoelastin fibers suggested distinct patterns of periodicity. As shown in Fig. 6, the periodicity of the waves of tropoelastin fibers electrospun at 1 ml/h was the smallest ( $71 \pm 28 \mu\text{m}$ ). By increasing the delivery rate, the periodicity increased to  $105 \pm 22 \mu\text{m}$  (at 3 ml/h) and was not significantly altered at higher delivery rates, (e.g.,  $126 \pm 25 \mu\text{m}$  at 7 ml/h). Analysis of the data by Student's *t*-test and single factor ANOVA indicated that there was no significant difference in the periodicity between 1 and 2 ml/h, nor from 3 to 9 ml/h ( $p > 0.05$ ), but there was a significant difference in the periodicity of the wave patterns between 2 and 3 ml/h ( $p < 0.05$ ). Upon further analysis of the data, the dependence of the periodicity on the delivery rate in Fig. 6 is optimally described by logarithmic regression ( $R^2 = 0.96$ ) rather than a linear regression ( $R^2 = 0.85$ ). The periodicity of tropoelastin fibers seemed to reach saturation above 3 ml/h. Based on

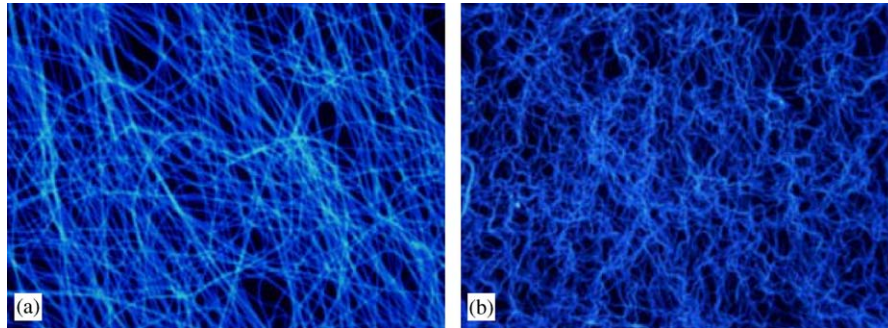


Fig. 5. Fluorescent images of electrospun (a) gelatin and (b) elastin fibers. The images show the autofluorescence of electrospun natural fibers. Images were acquired digitally using a Leica DMRX microscope equipped with a near UV filter cube with 340–380 nm excitation and 425 nm emission. Original magnification is  $100\times$ .

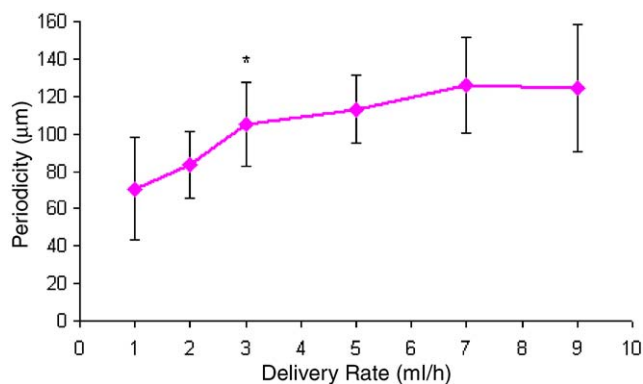


Fig. 6. Periodicities of electrospun tropoelastin fibers at different delivery rates. Digital SEM micrographs were analyzed using ImageTool3. Data are expressed as means  $\pm$  SD,  $n = 12$ . \*  $p < 0.05$ , values are significantly different from the previous group compared.

the above observation and discussion, our results open the possibility to use tropoelastin, or alpha-elastin, for fabricating engineered scaffolds comprised of wavy fibers which mimic the wavy topology of elastin in natural tissues such as elastic arteries.

For tissue engineering applications, bioartificial scaffolds are preferably porous, pliable, and elastic, so that cells will be able to integrate and/or push the ECM-like fiber aside as they grow into the scaffolds. One possible strategy for engineering tissue-like constructs is to emulate the mechanical and elastic properties of natural tissues by electrospinning composite scaffolds comprised of complex blends of collagen/gelatin and elastin/tropoelastin.

To examine the tensile property of the electrospun fibers, we performed microtensile test for these electrospun fiber sheets. Fig. 7 shows the strain–stress curves of 8% gelatin, 10% collagen, 20% tropoelastin, and 20% elastin. These concentrations were chosen for the production of bead-free fibers, based on our preliminary results. Also listed in this figure are the typical secondary

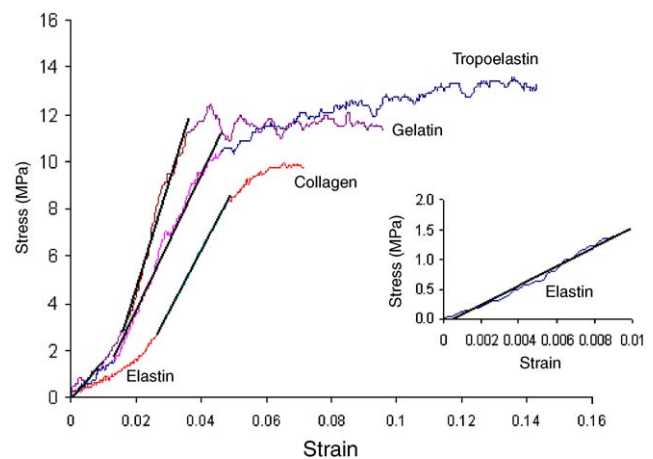


Fig. 7. Microtensile test of electrospun natural polymeric fibers. Compared are tensile strengths of 8% Gelatin, 10% Collagen, 20% Tropoelastin, and 20% Elastin fibers. For detail tensile moduli refer to Table 1.

Table 1  
Tensile moduli of electrospun protein fibers (MPa) ( $n = 3$ )

Gelatin	Collagen	Elastin	Tropoelastin
$426 \pm 39$	$262 \pm 18$	$184 \pm 98$	$289^a$

Only one sample was measured for recombinant human tropoelastin fibers due to the limited availability of the material precluded performing more tests.

<sup>a</sup>The limited availability of the recombinant material precluded performing these tests with tropoelastin.

tensile moduli. The average moduli are listed in Table 1. Electrospun collagen fibers have a lower tensile modulus than gelatin fibers, but have similar tensile strength (8–12 MPa) and ultimate elongation (0.08–0.1), respectively. Moreover, elastin fibers are much more brittle than gelatin and collagen, even tropoelastin fibers: the tensile strength of elastin fibers is only

about 1.6 MPa and the ultimate elongation is about 0.01. Tropoelastin is more elastic than elastin, and also more elastic than gelatin and collagen fibers: its ultimate elongation reaches 0.15 and the tensile strength reaches almost 13 MPa. By comparing their elastic properties, we surmise that tropoelastin is advantageous over elastin for fabricating engineered scaffolds, which could mimic the *in vivo* ECM environment. For tissue engineering applications, *i.e.*, to realistically emulate characteristics of natural tissues, the mechanical properties of gelatin fiber scaffolds will have to be enhanced, for example by co-spinning with other synthetic polymers, such as polylactic/polyglycolic acid (PLA/PGA), PLGA or by additional carbon nanotubes [44,45].

### 3.2. Cell–scaffold interactions

All 3-D scaffolds made from electrospun fibers of ECM proteins support attachment, migration, and proliferation of HEPM cells. As assessed by measuring cell proliferation using AB [35,36] and morphological staining with bis-benzimide (Hoechst 33258) and rhodamine phalloidin (for nuclei and cytoskeleton, respectively). The data in Fig. 8 depicts cell proliferation of HEPM cells on scaffolds made of alpha-elastin, tropoelastin, collagen, and gelatin and, for comparison, on the gold-standard tissue culture-treated polystyrene (TCPS). All data were normalized to the initial seeding density at day 0, as assessed 4 h after seeding. As seen in this figure, on day 2 HEPM growth on all the scaffolds is consistently at least equal to or (for elastin) slight higher than that on the TCPS controls. By day 6, there are significantly more cells on all the scaffolds ( $p < 0.05$ ) than on TCPS. This statement is especially true for alpha elastin and tropoelastin, where the statistical significance exceeds  $p < 0.01$ .

The increased cell numbers might reflect the three-dimensionality of the scaffolds and the fact that the cells grow not only on top of these scaffolds but also into them. As always, with these kinds of assays, we cannot rule out the remote possibility that an increase in AB fluorescence might not necessarily reflect merely a higher degree of proliferation but indicate also increased metabolic activity levels of the cells in response to the nature and topography of the fibrous scaffolds.

The morphology of HEPM cells growing on the scaffolds, as visualized by fluorescent staining of nuclei and cytoskeleton, was typical for these embryonic mesenchymal cells (Fig. 9). Interestingly, cells growing at low densities on the fibrous scaffolds elaborated a large number of pseudopodia, with which they attach to individual fibers. Importantly, HEPM cells attached, spread, migrated, and proliferated to confluence equally well on collagenous scaffolds as on the scaffolds made

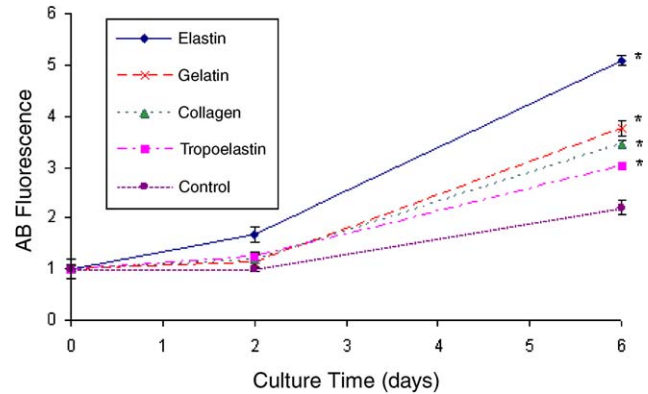


Fig. 8. HEPM cell proliferation on various substrates. HEPM cells were cultured on electrospun elastin, gelatin, collagen, tropoelastin and control TCPS substrates over a 6 day time course. Cell proliferation/metabolic activity were evaluated using the Alamar Blue (AB) Assay. The data were normalized to the AB fluorescence reading at day 0. Data are expressed as means  $\pm$  SD,  $n = 9$ . \*  $p < 0.05$ , values are significantly different from the control group.

from electrospun alpha-elastin and tropoelastin. These results warrant further investigations into the use of electrospun fibrous matrices, especially those made of or containing elastin and tropoelastin, for a large number of tissue engineering applications, such as for the building of high-fidelity functional cardiac, cardiovascular and pulmonary tissue constructs.

## 4. Conclusion

Electrospinning provides an efficient approach to fabricate biomimetic scaffolds from biopolymeric materials for tissue engineering. Since protein fibrils comprise a major structural and differentiating component of the ECM *in situ*, we surmise that the ideal engineered scaffolds will be those made from natural proteins which optimally emulate the mechanical and biochemical properties of natural, tissue-specific ECM. In this paper, we carefully evaluated how systematic variations of a number of experimental parameters of the electrospinning process affect the formation of proteinous fibers. Moreover, we characterized the basic physical fiber properties using SEM, AFM, and microtensile measurements. What is important to note is that recombinant human tropoelastin was electrospun for the first time and we observed the unique periodic wavy nature of electrospun alpha-elastin and tropoelastin fibers. The mechanical tensile properties of gelatin, collagen, alpha-elastin, and tropoelastin were measured and characterized. A limited set of cell culture studies demonstrates the usefulness of our fibrous scaffolds for cell attachment and proliferation and hence for potential widespread application in tissue engineering.

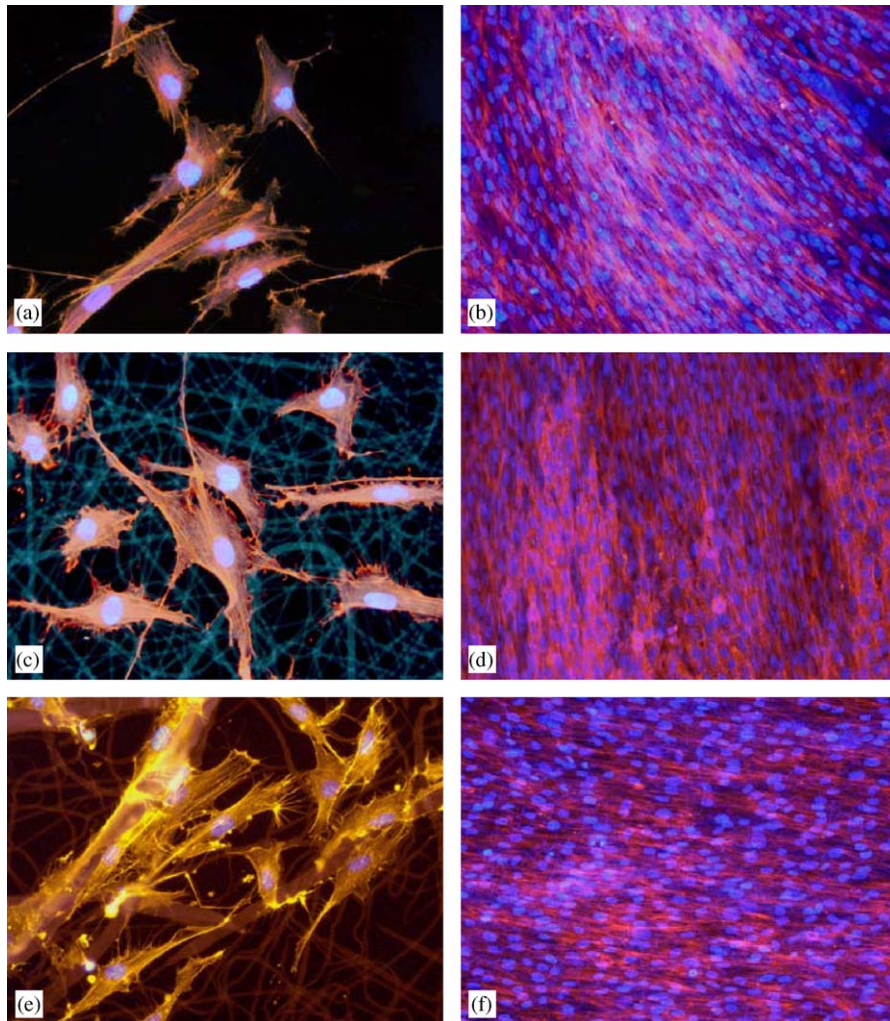


Fig. 9. Morphology of HEPM cells on protein fiber matrices. Staining for nuclei-bisbenzamide (blue), actin cytoskeleton-phalloidin (red), fibers-autofluorescence. HEPM cells attach, spread and form oriented monolayers on protein fiber matrices with typical fibroblastoid morphology. For details see Methods. (a,b) TCPS; (c,d) Gelatin; (e,f) Elastin; (a,c,e) HEPM after 48 h in culture (original magnification 400 ×); (b,d,f) HEPM monolayer at confluence after 72 h in culture (original magnification 200 ×).

## Acknowledgments

This work is supported by grants-in-aid from the Nanotechnology Institute of Southeast Pennsylvania (NTI, supporting ML and MG, with PIL and FKK are PIs) and NASA (NAG 2-1436, NNJ04HC81G-01, and NCC9-130, to PIL). MJM was supported, in part, through a Grant from NSF (Grant #DMI-0300405). We gratefully acknowledge NSF Award (BES-0216343) for the environmental scanning electron microscope (ESEM) and Dr. Guoliang Yang, Drexel University, for the use of the atomic force microscope. ASW was supported by Grants from the Australian Research Council and the University of Sydney Vice Chancellors Development Fund.

## References

- [1] Nishimura I, Garrell RL, Hedrick M, Iida K, Osher S, Wu B. Precursor tissue analogs as a tissue-engineering strategy. *Tissue Eng* 2003;9(Suppl 1):S77–89.
- [2] Larsen M, Tremblay ML, Yamada KM. Phosphatases in cell-matrix adhesion and migration. *Nat Rev Mol Cell Biol* 2003;4(9):700–11.
- [3] Iivanainen E, Kahari VM, Heino J, Elenius K. Endothelial cell-matrix interactions. *Microsc Res Tech* 2003;60(1):13–22.
- [4] Frame MC, Fincham VJ, Carragher NO, Wyke JA. v-Src's hold over actin and cell adhesions. *Nat Rev Mol Cell Biol* 2002;3(4):233–45.
- [5] Suzuki K, Saito J, Yanai R, Yamada N, Chikama T, Seki K, Nishida T. Cell-matrix and cell-cell interactions during corneal epithelial wound healing. *Prog Retin Eye Res* 2003;22(2):113–33.
- [6] Nguyen LL, D'Amore PA. Cellular interactions in vascular growth and differentiation. *Int Rev Cytol* 2001;204:1–48.

- [7] Baumgarten PK. Electrostatic spinning of acrylic microfibers. *J Colloid Interface Sci* 1971;36:71–9.
- [8] Bergshoef MM, Vancso GJ. Transparent nanocomposites with ultrathin, electrospun Nylon-4,6 fiber reinforcement. *Adv Mater* 1999;11(16):1362–5.
- [9] Jin HJ, Fridrikh SV, Rutledge GC, Kaplan DL. Electrospinning *Bombyx mori* silk with poly(ethylene oxide). *Biomacromolecules* 2002;3(6):1233–9.
- [10] Huang ZM, Zhang YZ, Kotaki M, Ramakrishna S. A review on polymer nanofibers by electrospinning and their applications in nanocomposites. *Composites Sci Technol* 2003;63:2223–53.
- [11] Buchko CJ, Chen LC, Shen Y, Martin DC. Processing and microstructural characterization of porous biocompatible protein polymer thin films. *Polymer* 1999;40:7397–407.
- [12] Min BM, Lee G, Kim SH, Nam YS, Lee TS, Park WH. Electrospinning of silk fibroin nanofibers and its effect on the adhesion and spreading of normal human keratinocytes and fibroblasts in vitro. *Biomaterials* 2004;25(7–8):1289–97.
- [13] Li WJ, Laurencin CT, Cateson EJ, Tuan RS, Ko FK. Electrospun nanofibrous structure: a novel scaffold for tissue engineering. *J Biomed Mater Res* 2002;60(4):613–21.
- [14] Kim K, Yu M, Zong X, Chiu J, Fang D, Seo YS, Hsiao BS, Chu B, Hadjiargyrou M. Control of degradation rate and hydrophilicity in electrospun non-woven poly(D,L-lactide) nanofiber scaffolds for biomedical applications. *Biomaterials* 2003;24:4977–85.
- [15] Bhattarai SR, Bhattarai N, Yi HK, Hwang PH, Cha DI, Kim HY. Novel biodegradable electrospun membrane: scaffold for tissue engineering. *Biomaterials* 2004;25:2595–602.
- [16] Katti DS, Robinson KW, Ko FK, Laurencin CT. Bioresorbable nanofiber-based systems for wound healing and drug delivery: optimization of fabrication parameters. *J Biomed Mater Res* 2004;70B(2):286–96.
- [17] Li WJ, Danielson KG, Alexander PG, Tuan RS. Biological response of chondrocytes cultured in three-dimensional nanofibrous poly(epsilon-caprolactone) scaffolds. *J Biomed Mater Res* 2003;67A(4):1105–14.
- [18] Yoshimoto H, Shin YM, Terai H, Vacanti JP. A biodegradable nanofiber scaffold by electrospinning and its potential for bone tissue engineering. *Biomaterials* 2003;24(12):2077–82.
- [19] Shin M, Yoshimoto H, Vacanti JP. In vivo bone tissue engineering using mesenchymal stem cells on a novel electrospun nanofibrous scaffold. *Tissue Eng* 2004;10(1–2):33–41.
- [20] Shin M, Ishii O, Sueda T, Vacanti JP. Contractile cardiac grafts using a novel nanofibrous mesh. *Biomaterials* 2004;25(17):3717–23.
- [21] Mo XM, Xu CY, Kotaki M, Ramakrishna S. Electrospun P(LLA-CL) nanofiber: a biomimetic extracellular matrix for smooth muscle cell and endothelial cell proliferation. *Biomaterials* 2004;25(10):1883–90.
- [22] Xu CY, Inai R, Kotaki M, Ramakrishna S. Aligned biodegradable nanofibrous structure: a potential scaffold for blood vessel engineering. *Biomaterials* 2004;25(5):877–86.
- [23] Khil MS, Cha DI, Kim HY, Kim IS, Bhattarai N. Electrospun nanofibrous polyurethane membrane as wound dressing. *J Biomed Mater Res* 2003;67B(2):675–9.
- [24] Toshima M, Ohtani Y, Ohtani O. Three-dimensional architecture of elastin and collagen fiber networks in the human and rat lung. *Arch Histol Cytol* 2004;67(1):31–40.
- [25] Ntayi C, Labrousse AL, Debret R, Birembaut P, Bellon G, Antonicelli F, Hornebeck W, Bernard P. Elastin-derived peptides upregulate matrix metalloproteinase-2-mediated melanoma cell invasion through elastin-binding protein. *J Invest Dermatol* 2004;122(2):256–65.
- [26] Lu Q, Ganesan K, Simionescu DT, Vyavahare NR. Novel porous aortic elastin and collagen scaffolds for tissue engineering. *Biomaterials* 2004;25(22):5227–37.
- [27] Buijtenhuijs P, Buttafoco L, Poot AA, Daamen WF, van Kuppevelt TH, Dijkstra PJ, de Vos RA, Sterk LM, Geelkerken BR, Feijen J, Vermes I. Tissue engineering of blood vessels: characterization of smooth-muscle cells for culturing on collagen- and elastin-based scaffolds. *Biotechnol Appl Biochem* 2004;39 (Pt 2):141–9.
- [28] Kim BS, Mooney DJ. Scaffolds for engineering smooth muscle under cyclic mechanical strain conditions. *J Biomech Eng* 2000;122(3):210–5.
- [29] Huang L, Nagapudi K, Apkarian RP, Chaikof EL. Engineered collagen-PEO nanofibers and fabrics. *J Biomater Sci Polym Ed* 2001;12:979–93.
- [30] Huang L, Apkarian RP, Chaikof EL. High-resolution analysis of engineered type I collagen nanofibers by electron microscopy. *Scanning* 2001;23:372–5.
- [31] Matthews JA, Wnek GE, Simpson DG, Bowlin GL. Electrospinning of collagen nanofibers. *Biomacromolecules* 2002;3(2):232–8.
- [32] Boland ED, Matthews JA, Pawlowski KJ, Simpson DG, Wnek GE, Bowlin GL. Electrospinning collagen and elastin: preliminary vascular tissue engineering. *Front Biosci* 2004;9:1422–32.
- [33] Vrhovski B, Weiss AS. Biochemistry of tropoelastin. *Eur J Biochem* 1998;258(1):1–18.
- [34] Martin SL, Vrhovski B, Weiss AS. Total synthesis and expression in *Escherichia coli* of a gene encoding human tropoelastin. *Gene* 1995;154(2):159–66.
- [35] Wu WJ, Vrhovski B, Weiss AS. Glycosaminoglycans mediate the coacervation of human tropoelastin through dominant charge interactions involving lysine side chains. *J Biol Chem* 1999;274(31):21719–24.
- [36] Yoneda T, Pratt RM. Interaction between glucocorticoids and epidermal growth factor in vitro in the growth of palatal mesenchymal cells from the human embryo. *Differentiation* 1981;19(3):194–8.
- [37] Nikolaychik VV, Wankowski DM, Samet MM, Lelkes PI. In vitro testing of endothelial cell monolayers under dynamic conditions inside a beating ventricular prosthesis. *ASAIO J* 1996;42(5):M487–94.
- [38] Nikolaychik VV, Samet MM, Lelkes PI. A new method for continual quantitation of viable cells on endothelialized polyurethanes. *J Biomater Sci Polym Ed* 1996;7(10):881–91.
- [39] Lelkes PI, Friedman JE, Rosenheck K, Oplatka A. Destabilization of actin filaments as a requirement for the secretion of catecholamines from permeabilized chromaffin cells. *FEBS Lett* 1986;308:375–83.
- [40] Fong H, Reneker DH. Electrospinning nanofibers of styrene-butadiene-styrene triblock copolymer. *J Polym Sci: Part B Polym Phys* 1999;37(24):3488–93.
- [41] Leppert PC, Yu SY. Three-dimensional structures of uterine elastic fibers: scanning electron microscopic studies. *Connect Tissue Res* 1991;27:15–31.
- [42] Birk DE, Silver FH, Trelstad RL. Matrix assembly. In: Hay ED, editor. *Cell biology of extracellular matrix*. 2nd ed. New York: Plenum Press; 1991. p. 221–54.
- [43] Basalyga DM, Simionescu DT, Xiong W, Baxter BT, Starcher BC, Vyavahare NR. Elastin degradation and calcification in an abdominal aorta injury model: role of matrix metalloproteinases. *Circulation* 2004;110(22):3480–7.
- [44] Weisenberger MC, Grulke EA, Jacques D, Rantell T, Andrews R. Enhanced mechanical properties of polyacrylonitrile/multiwall carbon nanotube composite fibers. *J Nanosci Nanotechnol* 2003;3(6):535–9.
- [45] Ko F, Gogotsi Y, Ali A, Naguib N, Ye H, Yang G, Li C, Willis P. Electrospinning of continuous carbon nanotube-filled nonfiber yarns. *Adv Mater* 2003;15(14):1161–5.